Contract No.:

This manuscript has been authored by Savannah River Nuclear Solutions (SRNS), LLC under Contract No. DE-AC09-08SR22470 with the U.S. Department of Energy (DOE) Office of Environmental Management (EM).

Benchmarking of Improved DPAC Transient Deflagration Analysis Code

James E. Laurinat[1]
Savannah River National Laboratory
Savannah River Site
Aiken, SC 29808
james.laurinat@srnl.doe.gov

Steve J. Hensel
Savannah River Nuclear Solutions
Savannah River Site
Aiken, SC 29808
steve.hensel@srs.gov
ASME Fellow

ABSTRACT

The deflagration pressure analysis code (DPAC) has been upgraded for use in modeling hydrogen deflagration transients. The upgraded code is benchmarked using data from vented hydrogen deflagration tests conducted at the HYDRO-SC Test Facility at the University of Pisa. DPAC originally was written to calculate peak deflagration pressures for deflagrations in radioactive waste storage tanks and process facilities at the Savannah River Site. Upgrades include the addition of a laminar flame speed correlation for hydrogen deflagrations and a mechanistic model for turbulent flame propagation, incorporation of inertial effects during venting, and inclusion of the effect of water vapor condensation on vessel walls. In addition, DPAC has been coupled with chemical equilibrium with applications (CEA), a NASA combustion chemistry code. The deflagration tests are modeled as end-to-end deflagrations. The improved DPAC code successfully predicts both the peak pressures during the deflagration tests and the times at which the pressure peaks.

[1] Corresponding author

INTRODUCTION

The deflagration pressure analysis code (DPAC) code originally was written to evaluate peak pressures for deflagrations in radioactive waste storage and process facilities at the Savannah River Site [1]. The primary purpose for the code was to provide a safety analysis method to address risks from hypothetical deflagrations. The original version of the code coupled a thermodynamic model of adiabatic isochoric complete combustion (AICC) for hydrogen/air and/or benzene/air mixtures with a simple flame propagation calculation. An option was added for flame propagation in one, two, or three dimensions. In lieu of a detailed thermal hydraulic model, the code simply divided the deflagration vessel into two volumes on either side of the flame front, one for unburned gas and the other for burned gas. The code included calculations for venting, radiative heat losses, and structural deformation due to pressurization from the deflagration. DPAC was written in standard Fortran and can be compiled to run on a personal computer.

Recently, there has been renewed interest in modeling hydrogen deflagrations. This interest, combined with the availability of additional data from vented hydrogen deflagration tests, provided motivation to modify DPAC.

The modified version of DPAC is limited to linear, end-to-end propagation of hydrogen/air deflagrations. This combination covers the majority of hypothetical deflagrations encountered in safety analyses. Upgrades to DPAC include the addition of a concentration-dependent laminar flame speed correlation, a model for turbulent enhancement of the flame speed, and the incorporation of inertial effects during the flame propagation. In the modified code, the thermodynamic calculations are performed by the NASA combustion code CEA [2,3], which is invoked within the Fortran executable. Structural analyses have been deleted, and a model for water vapor condensation on the vessel walls has been added.

Previous work on DPAC and the relationship of the code to other deflagration modeling work has been reviewed previously [1], so the following discussion focuses on the benchmark tests, the changes to DPAC, and a comparison of DPAC calculations with the benchmark test results.

DESCRIPTION OF BENCHMARK TESTS

A series of tests conducted using the HYDRO-SC Test Facility at the University of Pisa was selected for benchmarking of the deflagration calculations [4,5]. Carcassi and Fineschi conducted a series of unvented and vented tests in this facility, using 14% hydrogen in air. The HYDRO-SC test vessel was an upright cylindrical steel tank with a diameter of 0.650 m, a total height 1.628 m. The test vessel had top and bottom end caps, each with a radius of 0.520 m. Tests were conducted with an unvented tank and with 0.030-m, 0.05-m, 0.07-m, and 0.10-m diameter vents. The benchmarking calculations do not include any losses for these vents other than a 0.5 velocity head loss for a sudden flow entry. During the tests the gas mixture was ignited at the bottom of the tank, and the vent was located at the top. Consequently, these tests can be modeled using a model based on end-to-end flame propagation.

The Carcassi and Fineschi tests were chosen for benchmarking because they (1) used hydrogen gas in air, (2) were conducted using a tank that, although somewhat smaller than typical processing vessels or storage tanks, was representative in size, and (3) produced data for a range of vent sizes. In addition, an examination of the data indicates that the pressure transducers that were used had a sufficiently rapid response time to generate an accurate pressure profile. Fig. 1 depicts the pressure transients for the Carcassi and Fineschi tests.

OVERVIEW OF CHANGES TO DPAC

To obtain a better model to benchmark the pressure transients from the Carcassi and Fineschi tests, the DPAC source code was extensively revised. The most basic change was to the structure of the transient calculations within DPAC. In the preceding version, an energy balance was applied to simultaneously calculate the burning velocity and the rates of pressure and gas temperature changes due to burning, venting, and radiation heat transfer. In the modified version, these changes are calculated separately and consecutively at each calculation time step. This approach is valid if the time step is sufficiently small.

The flame speed is estimated by calculating the extent to which a burning flame compresses the unburned gas in the vessel. It is assumed that AICC takes place at the burning surface, and that the freshly burned gas then expands and simultaneously compresses both the unburned and previously burned gas in the vessel. Compression of the unburned and previously burned gases is assumed to occur adiabatically and isentropically, until the pressure of the freshly burned gas equals the vessel pressure.

A summary of other code modifications follows.

CHANGES TO COMBUSTION CALCULATIONS

The combustion calculation in DPAC is replaced by a call to an executable version of the NASA combustion code CEA [2,3]. CEA is used to compute gas properties both before and after combustion. The combustion is modeled as a constant volume combustion, so CEA gives the burned gas pressure and temperature prior to expansion into the volume occupied by the unburned gas. This expansion provides an acceleration factor to convert the turbulent burning velocity into an actual flame speed.

CHANGES TO LAMINAR BURNING VELOCITY

Previous versions of DPAC assigned the laminar burning velocity and the turbulent velocity multiplier as input items. In the modified version, an empirical laminar burning velocity correlation is added so that the laminar burning velocity can be calculated as a function of the temperature, the pressure, and the unburned gas composition. The correlation is fit to data compiled by Dahoe at difference hydrogen/air ratios for the unburned gas [6], as shown by Fig. 2.

The curve fit (see Fig. 2) takes the form

$$s_{L,s} = \left(\left(c_1 exp\left(c_2 \varphi \right) \right)^{c_5} + \left(c_3 \varphi^{c_4} \right)^{c_5} \right)^{\frac{1}{c_5}} \quad (1)$$

The empirical curve fit constants c_1, c_2, c_3, c_4, and c_5 have the values 4.216679, -0.2023, 2.217257, 1.425145, and -4.25637, respectively.

As recommended by Dahoe, the following correlation from Iijima and Takeno [7] is used to account for temperature and pressure changes:

$$s_L = s_{L,s} \left(\frac{T_0}{T_s} \right)^{1.4} \left(\frac{P_0}{P_s} \right)^{0.194} \quad (2)$$

CHANGES TO TURBULENT VELOCITY MULTIPLIER

The modified version of DPAC also includes a turbulence model to estimate the ratio of the turbulent burning velocity to the laminar burning velocity. The burning velocity prior to the expansion of the burned gas is estimated by combining an analysis conducted by Chen et al. [8], which gives the turbulent burning velocity as a function of the turbulence strength for the flame, with an estimate of the turbulence strength at the flame front. The Chen et al. correlation is an asymptotic combination of a turbulent diffusion model, originally proposed by Damköhler [9], and a limiting value for the turbulent flame speed obtained from experiments. The Damköhler model states that, for low level of turbulence, the flame front is thin. For thin flames, the turbulent flame speed is modeled as a function of the turbulent diffusivity, which in turn is proportional to the turbulence strength. Experiments with highly turbulent flames indicate that for thick flames, the increase in the turbulent burning velocity is due to the increase in the flame surface area caused by "wrinkling" of the flame front. This increase is limited to a value of twice the turbulence strength.

The Chen et al. correlation expresses the ratio of the difference between the turbulent burning velocity, s_T, and the laminar burning velocity, s_L, and the turbulence strength, v', as a function of the Damköhler number, Da_T.

$$\frac{s_T - s_L}{v'} = -\frac{a_4 b_3^{\,2} \mathrm{Da}_T}{2 b_1} + \left(\left(\frac{a_4 b_3^{\,2} \mathrm{Da}_T}{2 b_1} \right)^2 + a_4 b_3^{\,2} \mathrm{Da}_T \right)^{0.5} \quad (3)$$

The Damköhler number is defined in terms of the laminar burning velocity by scaling with the length scale for turbulent diffusion, L, the flame thickness, L_F, and the turbulence strength.

$$\mathrm{Da}_T = \frac{s_L L}{v' L_F} \quad (4)$$

The diffusion length scale and flame thickness are related by a proportionality constant, b_2.

$$L_F = b_2 L \quad (5)$$

The Chen et al. model is closed by using an approximate upper limit to the turbulence strength. For highly turbulent flow past a stationary conical flame,

experiments demonstrate that the turbulence strength reaches a maximum of approximately 20% of the maximum flow velocity past the flame [10]. This intensity level is in accord with typical values for different types of flows. With this approximation, the turbulence strength is related to the flame front velocity, v_T, by

$$v' = 0.2 v_T \tag{6}$$

CHANGES TO FLAME SPEED CALCULATION

One may assume that the total velocity at the flame front, without regard to direction of propagation, is limited to no more than the product of the turbulent burning velocity with respect to the moving flame front and the expansion factor for the burning gas. The expansion factor for the burning gas, in turn, is limited to the change in pressure as the gas expands from its maximum possible pressure for AICC to the vessel pressure. The flame velocity is obtained by multiplying the turbulent burning velocity by the ratio of the AICC pressure to the stagnation pressure (or actual pressure) in the vessel:

$$v_T = \left(\frac{P_{AICC}}{P_0} \right) s_T \tag{7}$$

The acceleration of the flame by expansion of the combustion gases is modeled by calculating the volume of unburned gas displaced as the burning gases expand from their AICC pressure to the pressure inside the vessel. The degree of acceleration depends on whether the flame behaves as a “confined” or a freely expanding flame. The rate of pressure increase for the Carcassi and Fineschi benchmark tests initially is high, indicating that the flame is “confined”, and later drops to a level consistent with that of a freely expanding flame. Separate flame acceleration factors are derived for “confined” and free flames.

The relative rates of pressure increase for confined and expanding flames can be compared by solving rate equations for each flame type. It is assumed that the rate of pressure increase for a confined flame is proportional to the pressure. In other words,

$$\frac{dP}{dt} = BP \tag{8}$$

The rate of pressure increase for a confined flame is given by the solution to this equation, which is

$$P = P_i \, exp\left(Bt \right) \tag{9}$$

For an expanding flame, the equation for the rate of pressure increase includes a propagation term that depends on the flame speed. In addition, the inherent rate of increase BP is multiplied by the ratio of the burned gas volume to its value at the transition from a confined flame to account for the decrease in pressure as the burned volume expands; this effectively makes the inherent rate increase constant. The expanding flame pressure transient equation takes the form

$$\frac{dP}{dt} = -\left(\frac{A_F v_F}{V_P} \right) P + \left(\frac{V_{P,tr}}{V_P} \right) BP \tag{10}$$

An additional equation can be written that relates the rate of change of the burned gas volume to the flame speed.

$$\frac{dV_P}{dt} = A_F v_F \tag{11}$$

The preceding two equations combine to yield

$$\frac{dPV_P}{dt} = BPV_{P,tr} \tag{12}$$

The transient pressure equation for the expanding flame also can be written for a Lagrangian reference frame that follows the flame front. In terms of the substantial derivative D, this equation is

$$\frac{DP}{Dt} = \left(\frac{V_{P,tr}}{V_P}\right) BP \tag{13}$$

Eq. (13) can be differentiated to get

$$\frac{D^2P}{Dt^2} = \frac{D}{Dt}\left(\left(\frac{V_{P,tr}}{V_P}\right) BP\right) \tag{14}$$

Previously, it was mentioned that the rate increase term for the expanding flame is constant, since any increase in pressure is balanced by a decrease in the burned gas volume. Thus,

$$\frac{D}{Dt}\left(\left(\frac{V_{P,tr}}{V_P}\right) BP\right) = 0 \tag{15}$$

and

$$\frac{D^2P}{Dt^2} = 0 \tag{16}$$

Because the pressure is assumed to be uniform within the burned gas volume, the substantial derivatives in Eqs. (15) and (16) may be replaced with ordinary derivatives to give

$$\frac{d}{dt}\left(\left(\frac{V_{P,tr}}{V_P}\right) BP\right) = 0 \tag{17}$$

and

$$\frac{d^2P}{dt^2} = 0 \tag{18}$$

Eqs. (12) and (17) now can be combined to yield the following solution for the rate of pressure increase.

$$\frac{dP}{dt} = \frac{1}{2}\left(\frac{V_{P,tr}}{V_P}\right) BP \tag{19}$$

From Eq. (18), the inherent rate of pressure increase, i.e., the right side of Eq. (19), must be constant. Therefore, for an expanding flame,

$$\frac{dP}{dt} = \frac{1}{2} BP_{tr} \tag{20}$$

where P_{tr} is the pressure at the transition from a confined to an expanding flame. A comparison of Eqs. (8) and (20) shows that the rate of pressure increase for an expanding flame is half that for a confined flame.

The transition from a confined flame to an expanding flame is applied when the resistance to expansion into the volume of unburned gas in the vessel becomes equal to the resistance to expansion into the burned gas. This is assumed to occur when the numbers of moles of unburned and burned gas remaining in the vessel are equal.

The flame speed calculation sets the flame speed (with respect to a fixed location) equal to the product of the burning velocity (the velocity at which the unburned gas flows into the flame) and a volume ratio for expansion of the gas that has burned during the current time step. It is assumed that the gas expands until its pressure equilibrates with the pressure in the vessel. The starting pressure prior to expansion is set equal to the AICC pressure. To ensure that the final vessel pressure for complete combustion will reach the AICC pressure (not accounting for heat losses), the volumetric expansion calculations are based on simple, constant temperature volumetric displacement rather than isentropic expansion and compression. It is recognized that this simplistic approach may lead to errors in temperature calculations, but the approach is deemed adequate for calculating pressure transients.

CHANGES TO VENTING ANALYSIS

An exact, iterative calculation of the venting flow rate replaces the semi-empirical estimate of venting flow rates for non-choking flow. As in the previous versions of DPAC, the flow out the vents is assumed to be at steady state with respect to the relatively slower combustion transient. The vent flow is modeled using equations for isentropic flow [11], which are solved iteratively. The relative venting rates of unburned and burned gases are proportioned by the relative volumes of unburned and burned gases remaining in the vessel; this apportioning was also used in previous versions of DPAC.

Inertial effects are added to better model the well-vented benchmark tests. The pressure transients for the 0.070-m and 0.10-m vent tests exhibit rapid initial rates of increase that can be explained by assuming that gases do not vent from the vessel until a threshold pressure has been reached. If it is assumed that the initiation of venting requires the establishment of choked flow through the vents, then the threshold pressure is the stagnation pressure required to establish choked flow in the vents. Accordingly, the threshold pressure increase before venting starts is set at the stagnation pressure for choked flow, so that there is no venting while

$$\frac{P}{P_i} \le \frac{P_0}{P_2} \tag{21}$$

where P_i is the initial pressure in the vessel and the ratio on the right side of the equation is the ratio of the stagnation pressure to the exit pressure, given by

$$\frac{P_0}{P_2} = \left(\frac{k_R + 1}{2} \right)^{\frac{k_R}{k_R - 1}} \tag{22}$$

The maximum vent area for an initial shock can be estimated by comparing the measured initial rate of pressure increase for an unvented deflagration to the rate of pressure decrease due to venting. The rate of pressure change due to venting can be derived from a mass balance for the contents of the vessel. The mass balance is applied to conditions just after ignition, so it uses the properties for the unburned gas. The mass balance takes the form

$$V\frac{D\rho_R}{Dt} = -A_v \rho_R v_{out} \tag{23}$$

where v_{out} is the velocity out the vent, at the inlet temperature and pressure.

It may be noted that the mass balance is expressed in terms of the substantial derivative. This is done to include inertial nonequilibrium terms, so that the analysis is applied to a shock wave that propagates back into the vessel from the vent.

The density change in the mass balance is converted to a pressure change by assuming that the flow out the vent occurs isentropically. For isentropic changes,

$$\frac{1}{\rho_R}\frac{D\rho_R}{Dt} = \frac{1}{k_R P}\frac{DP}{Dt} \tag{24}$$

As explained previously, the substantial derivative yields a pressure change that is half that given by the ordinary derivative. Thus,

$$\frac{DP}{Dt} = \frac{1}{2}\frac{dP}{dt} \tag{25}$$

and

$$\left(\frac{1}{P}\frac{dP}{dt}\right)_{out} = -\left(\frac{2k_R A_v v_{out}}{V}\right) \tag{26}$$

where $\left(\frac{1}{P}\frac{dP}{dt}\right)_{out}$ represents the normalized rate of pressure change due to flow out the vent.

The criterion for the maximum size vent for which venting begins without an initial wait period is obtained by setting this rate of pressure change equal to the calculated rate of pressure change for an unvented deflagration,

$$\left(\frac{1}{P}\frac{dP}{dt}\right)_{out} + \left(\frac{1}{P}\frac{dP}{dt}\right)_{def} = 0 \tag{27}$$

The criterion, then, is

$$\left(\frac{1}{P}\frac{dP}{dt}\right)_{def} \geq \frac{2k_R A_v v_{out}}{V} \tag{28}$$

For vent areas less than the area calculated by this expression, a transient shock will not form at the vent, and venting will start immediately after ignition. For larger areas, a shock will develop, and venting will be delayed until the pressure increases to the value specified by Eq. (21).

The outlet velocity is estimated as being equal to the sonic velocity for the unburned gas in the vessel, $\left(k_R R_g T_{R,i}\right)^{0.5}$, and the Mach number, M_s:

$$v_{out} = \mathrm{M}_s \left(\frac{k_R R_g T_{R,i}}{M_g} \right)^{0.5} \tag{29}$$

The exit Mach number is equal to the ratio of the stagnation pressure to the exit pressure, which is given by

$$\mathrm{M}_s = \left(\frac{2}{k_R + 1} \right)^{\frac{1}{k_R - 1}} \tag{30}$$

Venting also can affect how the flame front propagates later during the deflagration transient. When the deflagration undergoes the transition from a confined flame to an expanding flame, venting is capable of accelerating the propagation of the flame so that a greater portion of the unburned gases are vented before they burn. The effective velocity for acceleration of the flame front is calculated by subtracting the equivalent venting velocity for the unburned gas from the equivalent velocity of the burned gas. The equivalent velocity is obtained by dividing the volumetric vent flow rate by the flame front area. If this velocity is greater than the flame speed, then the flame is accelerated by venting. As just described, the criterion for flame acceleration by venting is that

$$-\left(\frac{1}{\rho_P} \frac{dm_P}{dt} - \frac{1}{\rho_R} \frac{dm_R}{dt} \right) > A_F v_F \tag{31}$$

CHANGES TO HEAT TRANSFER ANALYSIS

DPAC models the thermal radiation that occurs between the hot combustion product gases to the cooler walls of the vessel. Thermal radiation is emitted by the water vapor in the burned gas; the oxygen and nitrogen in both the unburned and burned gases do not emit or absorb thermal radiation and therefore do not participate in radiation heat transfer. In the previous versions of DPAC, the temperature transients of both the combustion product gases and the vessel walls were calculated. For the modified version of DPAC, it is assumed that the vessel wall temperatures are much lower than the burned gas temperature, so that the rate of heat transfer is approximately equal to the rate of thermal radiation to a vacuum. This assumption decouples the analysis of the wall temperature from the gas heat transfer problem; consequently, a wall temperature calculation is not included in the modified code. The thermal radiation heat transfer rate is calculated using the simplified form of the Stefan-Boltzmann equation for radiation to a vacuum, which takes the form

$$q_{rad} = \varepsilon_{eff} \sigma A F_A T_P^{\,4} \tag{32}$$

The effective emissivity is given as a function of the surface emissivities for the burned gas and the vessel surface by the formula

$$\varepsilon_{eff} = \frac{1}{\frac{1}{\varepsilon_{gas}} + \frac{1}{\varepsilon_{surf}} - 1} \tag{33}$$

The emissivity for the vessel surface is assumed to be that for an oxidized steel surface at ambient temperature, which is approximately 0.8.

The previous version of DPAC used an empirical fit to the emissivity measurements reported by Hottel and Sarofim [12]. In the modified version, the correlation of Cess and Lian [13] is used to calculate the burned gas emissivity. Their correlation represents a fit to the data of Hottel and Sarofim over a wide range of temperatures that covers the conditions for the combustion of ambient air. The correlation takes the form

$$\varepsilon_{gas} = 0.691\left(1 - exp\left(-1.25\left(\frac{P_{H_2O}P_{eff}L_{\varepsilon}}{P_a^{\,2}}\left(\frac{300}{T_P}\right)\right)^{0.5}\right)\right) \tag{34}$$

where P_{eff} is the effective pressure representing water vapor radiation absorption band broadening by air and L_{ε} is the characteristic length for thermal radiation in vessel. The characteristic radiation length is assumed to be equal to 3.5 times the gas space volume, divided by the interior surface area [14].

The effective pressure, P_{eff}, from the work of Edwards and Balakrishnan [15], is expressed as

$$P_{eff} = P - P_{H_2O} + P_{H_2O}\left(0.5 + 5\left(\frac{300}{T_P}\right)^{0.5}\right) \tag{35}$$

The view factor F_A is equal to the outer surface area of the burned gases divided by the total vessel surface area. In the analysis, it is assumed that, if ignition occurs in one end of a cylindrical vessel, the burned gases will fill that end as the combustion front propagates. This implies that the view factor is given by the ratio of the surface area of the vessel filled with burned gases to a certain height, divided by the total surface area. The formula for the ratio of these two surface areas reduces to a function of the volume fraction of space occupied by burned gas, V_F, and the ratio of the gas space height, h_g, to the vessel diameter, d_t, given by

$$F_A = \frac{1 + 2V_F\left(\frac{h_g}{d_t}\right)}{1 + 2\left(\frac{h_g}{d_t}\right)} \tag{36}$$

DPAC also is altered to account for the enhancement of radiative heat transfer due to droplet condensation from the combustion product gas. Condensation significantly affects the heat transfer rate and pressure drop only after combustion is complete and all unburned gases have been purged from the vessel. If any noncondensable gases (i.e., nitrogen mixed with unburned oxygen and hydrogen) remain in the vessel, they will form an inert gas barrier that will prevent rapid film condensation from occurring. Once the noncondensable gases are no longer present, condensation effectively accelerates the thermal radiation heat transfer. The

acceleration takes place as gas displaces the condensing water vapor at the vessel surface. The radiative heat transfer rate is enhanced by a ratio equal to the latent heat content of the gas divided by the pressure-volume work required to expand the gas to displace the condensed vapor. Thus,

$$q_{rad,c} = q_{rad} + q_c = q_{rad}\left(1 + \frac{x_{H_2O}\Delta h_{vap}}{R_g\left(T_P - T_0\right)}\right) \tag{37}$$

Condensation also affects the discharge rate by removing water vapor that must be displaced, thereby significantly increasing the rate of pressure loss for a given discharge rate. The magnitude of the condensation effect is given by

$$\Delta P_{c,tot} = \Delta P\left(1 + \frac{x_{H_2O}}{k_P - 1}\right) \tag{38}$$

COMPARISON OF DPAC CALCULATIONS WITH BENCHMARK DEFLAGRATION TRANSIENTS

Figs. 3-5 compare deflagration transients calculated by the modified version of DPAC with the measurements of Carcassi and Fineschi. Transients are compared for the no venting case (Fig. 3), the smallest vent (Fig. 4), and the largest vent (Fig. 5). The predicted deflagration transients shown in these figures fairly closely match the measured transients, with respect to both the peak pressure and the rate of pressure change during the deflagration and subsequent venting. Although DPAC provides an accurate estimate of the overall rate for the deflagration transient, the initial rates of pressure increase calculated by DPAC exceed the measured rates. This probably is due to the fact that the DPAC model assumes that the flame front starts as a planar front that covers the entire bottom surface of the vessel, whereas an actual flame probably ignites over a small surface area. This implies that the initial rate of pressure should be lower than calculated, until the flame spreads to cover the entire cross-section of the vessel.

The comparison for the unvented test provides a check of the accuracy of the thermal radiation and condensation heat transfer models within DPAC. As Fig. 3 shows, without any heat losses the pressure in the vessel increases until it reaches the AICC pressure of 5.448 bar. With heat losses included, the predicted peak pressure is 4.702 bar, compared to a measured peak pressure of 4.507 bar. This comparison indicates that the DPAC predictions are slightly conservative in that they underestimate the amount of heat loss.

For the vented tests, the comparisons also indicate how well DPAC models the effect of venting. DPAC accurately predicts the pressure transients for the two smaller vents, as illustrated by Fig. 4. The predicted pressure transients for the two larger vents did not agree with the measured transients until inertial effects are included, as Fig. 5 demonstrates. As stated previously, one inertial effect is the development of a pressure shock that propagates backward from the vent into the vessel for sufficiently large vents, and a second effect is the acceleration of the flame front by venting, again for large vents. The DPAC code models the first effect by suppressing venting until the

vessel pressure reaches the minimum value for sonic flow through the vents. DPAC accounts for the second effect by allowing complete venting of the unburned gases when the difference between the vent flow rates, scaled to the flame front area, first exceeds the flame speed. With these changes, DPAC generates a better estimate of the peak pressure and a better estimate of the rate of venting pressure losses for the 100 mm vent.

Table 1 summarizes the comparison of measured and calculated peak pressures and venting rates for the Carcassi and Fineschi tests. It may be seen that the modified version of DPAC accurately predicts the peak pressures and the deflagration times required to reach the peaks, when inertial effects are included to model the two tests with the largest vents.

SUMMARY AND CONCLUSIONS

The DPAC transient deflagration code has been modified and successfully benchmarked using a series of vented deflagration tests performed at the University of Pisa. The modified version of DPAC serves as a tool to predict maximum pressures for safety analyses of hypothetical hydrogen deflagrations at the Savannah River Site. Modifications to DPAC include the addition of a laminar burning velocity correlation and a mechanistic model for the turbulent burning velocity multiplier, improvement of the modeling of radiative heat transfer, incorporation of a model for condensate heat transfer, and the inclusion of inertial effects in the calculation of the flame speed. The benchmarking studies demonstrated that the inertial effects play a significant role in determining the rate of pressure rise and are needed to successfully model well-vented deflagrations.

Several features present in previous versions of DPAC were judged to be of minor use in addressing current safety analysis concerns and therefore were deleted. The modified version of DPAC no longer performs combustion chemistry calculations for gas mixtures other than hydrogen and air and does not include any structural analyses or wall temperature calculations. In addition, the code is restricted to the modeling of one-dimensional, end-to-end flame propagation. Even with these limitations, it is anticipated that DPAC will be able to address most safety analysis needs.

DPAC is configured as a Fortran executable on a personal computer platform. A code user is required to use an input text file. Use of the code requires the presence of an executable copy of Version 2 of the NASA combustion code CEA on the same platform or at an addressable location.

ACKNOWLEDGMENT

This manuscript has been authored by Savannah River Nuclear Solutions, LLC under contract number DE-AC09-08SR22470.

FUNDING

U. S. Department of Energy (Contract No. DE-AC09-08SR22470).

NOMENCLATURE

A	vessel interior surface area, m^2
A_F	flame front area, m^2
A_v	cross-sectional flow area of the vent, m^2
a_4	turbulent diffusivity coefficient, 0.78
b_1	limiting ratio of turbulent burning velocity to turbulence intensity, 2.0
b_2	proportionality constant, 1.78
b_3	coefficient for the relative increase in the ratio of the turbulent and laminar burning velocities as a function of the square root of the ratio of the turbulent and laminar diffusivities, 1.0
c_i	empirical curve fit parameters for Dahoe laminar flame speed measurements (i = 1 to 5)
B	arbitrary proportionality constant
d_t	vessel diameter, m
Da_T	Damköhler number for turbulent flames
F_A	fraction of the vessel surface area that receives radiation, equivalent to a viewing factor
h_g	height of the total gas space in the vessel, m
Δh_{vap}	molar heat of vaporization for water at the surface temperature, J/mol
k_P	heat capacity ratio for burned gas, J/mol/K
k_R	heat capacity ratio for unburned gas, J/mol/K
L	length scale for turbulent diffusion across the flame, m
L_F	flame thickness, m
L_ε	characteristic length for thermal radiation in the vessel, m
m_P	mass of burned gas in the vessel, kg
m_R	mass of unburned gas in the vessel, kg
M_g	molecular mass of gas, kg/mol
M_s	Mach number at stagnation conditions
P	pressure in the vessel, Pa
P_a	atmospheric pressure, 0.1013 MPa
P_{AICC}	pressure for adiabatic, isochoric complete combustion (AICC), Pa
P_{eff}	effective pressure representing water vapor radiation absorption band broadening by air, Pa
P_{H_2O}	water vapor partial pressure, Pa
P_i	initial pressure in the vessel, Pa
P_s	standard pressure for the laminar burning velocity correlation, 0.1 MPa (1 bar)

P_{tr}	pressure at the transition from a confined to an expanding flame, Pa
P_0	stagnation pressure, Pa
P_2	exit pressure, Pa
ΔP	change in pressure without including the effect of condensation, Pa
$\Delta P_{c,tot}$	total change in pressure for venting of burned gas, including the effect of condensation on the vessel walls, Pa
q_c	condensation heat transfer rate, W/m^2
q_{rad}	thermal radiation heat transfer rate, W/m^2
$q_{rad,c}$	total heat transfer rate including thermal radiation and condensation, W/m^2
R_g	ideal gas law constant, 8.314 J/mol/K
s_L	laminar burning velocity in Lagrangian coordinates (following the flame front), m/s
$s_{L,s}$	laminar burning velocity at standard temperature (300 K) and pressure (0.1 MPa or 1.0 bar), m/s
s_T	turbulent burning velocity in Lagrangian coordinates (following the flame front), m/s
t	time, s
Δt	time step, s
T_P	product gas temperature for constant pressure complete combustion, K
$T_{R,i}$	initial unburned gas temperature, K
T_s	standard temperature for the laminar burning velocity correlation, 300 K
T_0	temperature of unburned gas, stagnation temperature, K
v'	turbulence strength, m/s
v_F	flame speed, m/s
v_{out}	velocity out the vent, at the inlet temperature and pressure, m/s
v_T	total velocity at the flame front, m/s
V	vessel volume, m^3
V_F	fraction of the vessel gas space occupied by burned gas
V_P	burned gas volume, m^3
$V_{P,tr}$	burned gas volume at the transition from a confined to an expanding flame, m^3
x_{H_2O}	mole fraction of water vapor in the burned gas
ε_{eff}	effective emissivity for the burned gas
ε_{gas}	emissivity of the burned gas
ε_{surf}	emissivity of the vessel surface
ρ_P	burned gas density, kg/m^3

ρ_R	unburned gas density, kg/m^3
σ	Stefan-Boltzmann constant, 5.671E-08 W/m^2/K^4
φ	hydrogen equivalency ratio, equal to the hydrogen molar concentration divided by twice the oxygen molar concentration

REFERENCES

[1] Hensel, S. J., and Thomas, J. K., 1994, "Development and Application of a Deflagration Pressure Analysis Code for High Level Waste Processing," ASME Paper 941142-9.

[2] Gordon, S., and McBride, B. J., 1994, "Computer Program for Calculation of Complex Chemical Equilibrium Compositions and Applications: I. Analysis," NASA Lewis Research Center, Cleveland, OH, Technical Report No. 1311.

[3] McBride, B. J., and Gordon, S., 1996, "Computer Program for Calculation of Complex Chemical Equilibrium Compositions and Applications: II. Users Manual and Program Description," NASA Lewis Research Center, Cleveland, OH, Technical Report No. NASA RP-1311-P2.

[4] Carcassi, M. N., and Fineschi, F., 1993, "A Theoretical and Experimental Study on the Hydrogen Vented Deflagration," Nucl. Eng. Des., **145**(3), pp. 355-364.

[5] Carcassi, M. N., Fineschi, F., and Lombardi, G., 1987, "Air-Hydrogen Deflagration Tests at the University of Pisa," Nucl. Eng. Des., **104**(3), pp. 241-247.

[6] Dahoe, A. E., 2005, "Laminar Burning Velocities of Hydrogen-Air Mixtures from Closed Vessel Gas Explosions," J. Loss Prevent. Proc., **18**(3), pp. 152-166.

[7] Iijima, T., and Takeno, T., 1986, "Effects of Temperature and Pressure on Burning Velocity," Combust. Flame, **65**(1), pp. 35-43.

[8] Chen, M., Herrmann, M., and Peters, N., 2000, "Flamelet Modeling of Lifted Turbulent Methane/Air and Propane/Air Jet Diffusion Flames," P. Combust. Inst., **28**(1), pp. 167-174.

[9] Damköhler, G., 1940, "Der Einfluss der Turbulenz auf die Flammengeschwindigkeit in Gasgemischen," Z. Elektrochem., **46**(11), pp. 601-626 (English translation, NASA Technical Memorandum 1112, 1947).

[10] Griebel, P., Schären, R., Siewert, P., Bombach, R., Inauen, A., and Kreutner, W., 2003, "Flow Field and Structure of Turbulent High-Pressure Premixed Methane/Air Flames," ASME Paper No. GT2003-38398.

[11] Levenspiel, O., 1977, “The Discharge of Gases from a Reservoir through a Pipe,” AIChE J., **23**(3), pp. 402-403.

[12] Hottel, H. C., and Sarofim, A. F., *Radiative Transfer*, McGraw-Hill, New York (1967), pp. 225-258.

[13] Cess R. D., and Lian, M. S., 1976, “A Simple Parameterization for the Water Vapor Emissivity,” J. Heat Transfer, **98**(6), pp. 676-678.

[14] Siegel, R., and Howell, J. R., 1981, *Thermal Radiation Heat Transfer*, Hemisphere, New York.

[15] Edwards, D. K., and Balakrishnan, A., 1973, “Thermal Radiation by Combustion Gases,” Int. J. Heat Mass Transfer, **16**(1), pp. 25-40.

Fig. 1. Pressure transients for Carcassi and Fineschi deflagration tests

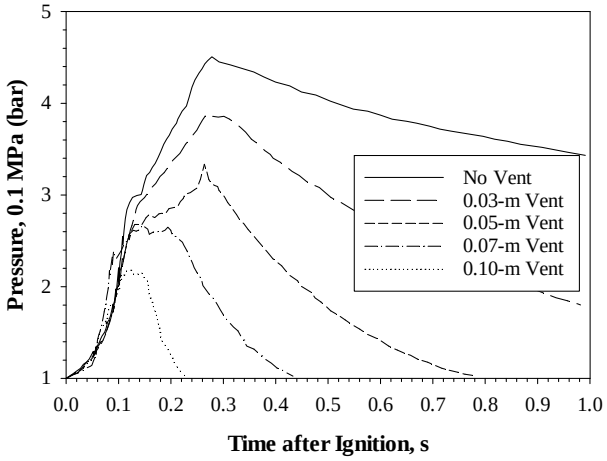

Fig. 2. Correlation of laminar burning velocities

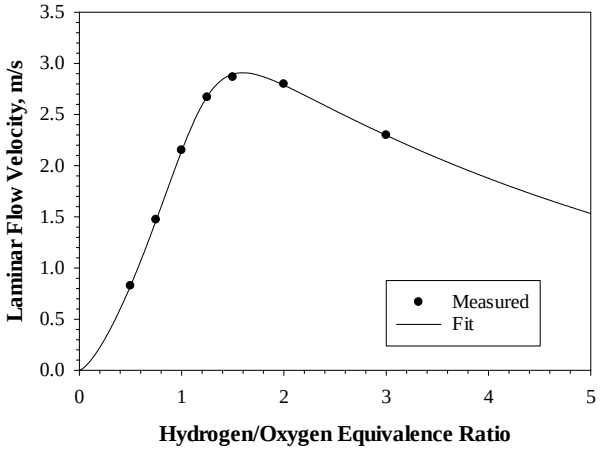

Fig. 3. Modeling of pressure transient for Carcassi and Fineschi unvented test

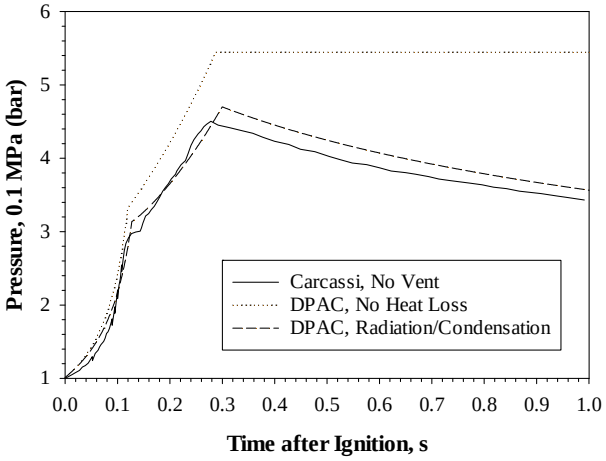

Fig. 4. Modeling of pressure transient for Carcassi and Fineschi 0.03 m vent test

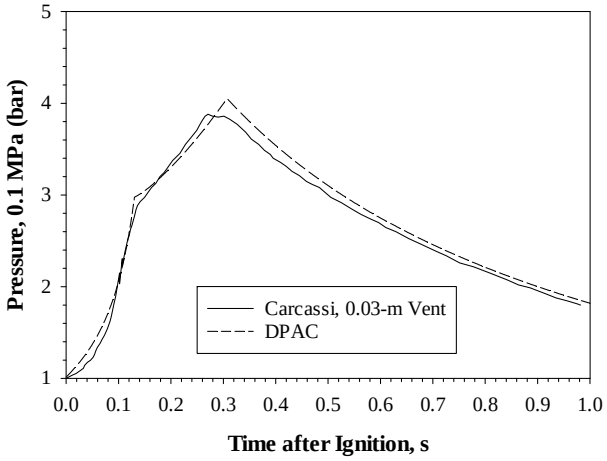

Fig. 5. Modeling of pressure transient for Carcassi and Fineschi 0.10 m vent test

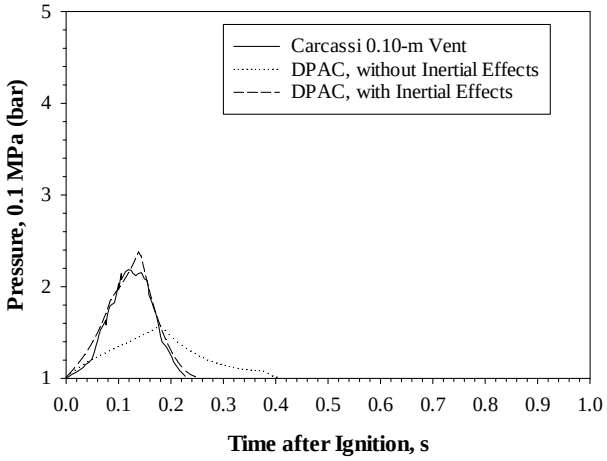

Table 1 Comparison of measured and calculated peak pressures for Carcassi and Fineschi deflagration tests

Vent diameter (m)	Measured peak press. (0.1 MPa, bar)	Measured time to Peak (s)	Calculated peak press.[a] (0.1 MPa, bar)	Calculated time to Peak (s)
No vent	4.507	0.278	4.702	0.300
0.03	3.882	0.271	4.053	0.307
0.05	3.334	0.264	3.081	0.320
0.07	2.670	0.145	2.761	0.131
0.10	2.187	0.119	2.382	0.138

[a] The calculated peak pressures for the 0.070-m and 0.10-m vent tests account for inertial effects associated with propagation of a pressure shock back from the vent during the initial stages of the transient and with subsequent acceleration of the flame front due to venting.